Turkish Journal of Earth Sciences

http://journals.tubitak.gov.tr/earth/

Research Article

Turkish J Earth Sci
(2020) 29: 347-362

doi:10.3906/yer-1907-8

Excess lifetime cancer risk due to natural radioactivity in Gümüşhane Province, NE Turkey

Nafiz MADEN[1,*], Enver AKARYALI[2], Mehmet Ali GÜCER[2]
[1]Department of Geophysics, Gümüşhane University, Gümüşhane, Turkey
[2]Department of Geology, Gümüşhane University, Gümüşhane, Turkey

Received: 04.07.2019 • **Accepted/Published Online:** 07.11.2019 • **Final Version:** 15.01.2020

Abstract: In this study, 162 in situ measurements of ^{238}U, ^{232}Th, and ^{40}K radionuclide concentrations dataset taken by the gamma-ray spectrometer in Gümüşhane, Turkey are presented. The gamma ray measurements were performed by a 512-channel, three-window gamma-ray spectrometry equipment made by GF Instruments. We first observed the radionuclides of the ^{238}U, ^{232}Th, and ^{40}K values in Gümüşhane. We then calculated the hazard indices of gamma radiation such as annual effective dose equivalent (AEDE), internal and external hazard index (H_{in}, H_{ex}), and excess lifetime cancer risk (ELCR) based on the radionuclide abundances of ^{238}U, ^{232}Th, and ^{40}K for the first time. In Gümüşhane, the average activity concentrations of radionuclides ^{238}U, ^{232}Th, and ^{40}K were measured as 58.7 ± 34.3 Bq kg^{-1}, 62.7 ± 37.2 Bq kg^{-1}, and 1026.8 ± 486.0 Bq kg^{-1}, respectively. The average outdoor annual effective dose equivalent and ELCR values were 132.2 ± 63.2 mSv yr^{-1} and 0.40 ± 0.19 × 10^{-3}, respectively. Numerical results indicate that the radiological parameters (AEDE and ELCR) obtained for Gümüşhane Province were greater than the world's mean values.

Key words: Annual effective dose equivalent, internal hazard index, excess lifetime cancer risk, Gümüşhane

1. Introduction

The method of gamma-ray spectrometry provides information about ELCR utilizing the radionuclides of the ^{238}U, ^{232}Th, and ^{40}K values in granites, soils, and sediments (Chen and Lin, 1996; Karakelle et al., 2002; Pavlidou et al., 2006). In Turkey, a few number of studies have been carried out in the area of ELCR (Karahan and Bayülken, 2000; Örgün et al., 2005; Merdanoğlu and Altınsoy, 2006; Kam and Bozkurt, 2007; Kurnaz et al., 2007; Değerlier et al., 2008; Kılıç et al., 2008; Kalyoncuoğlu et al., 2015; Küçükömeroğlu et al., 2016; Maden et al., 2019).

The natural gamma radiation due to the terrestrial radionuclides was investigated using the radionuclide concentrations gathered from 105 soil samples from locations in both urban and rural environments of İstanbul Province (Karahan and Bayülken, 2000). Taşkın et al. (2009) determined the ELCR using $AEDE_{out}$ in Kırklareli.

Kobya et al. (2015) computed AEDE and ELCR utilizing $AEDE_{out}$ values to evaluate the background radiation level and public health hazards in Artvin Province. Küçükömeroğlu et al. (2016) determined the radiological hazard indices in beach sands along the Trabzon, Giresun, and Ordu coastal regions. Durusoy and Yıldırım (2017) measured the radionuclides activity concentrations in 24 soil samples from the study region by using gamma ray spectrometry. Kapdan et al. (2018) determined the soil radioactivity levels and assessed the possible relevant health hazards for the inhabitants of Ankara Province. Maden et al. (2019) evaluated the radiological hazards indices using the ^{40}K, ^{238}U, and ^{232}Th radionuclide concentrations in 48 stations taken by the γ-ray spectrometer in Gümüşhane Province.

This research attempts to identify the radiological hazard indices measuring the concentration of ^{238}U, ^{232}Th, and ^{40}K radioisotopes taken by the gamma-ray spectrometry equipment in Gümüşhane, Turkey. Herein the ELCR is presented to appreciate the health hazards in Gümüşhane. This is the first study in which the ELCR is obtained with the AEDE values gathered from 162 different locations in Gümüşhane.

2. Geological background

Turkey was geologically created during the Alpine orogeny in which mostly ophiolites, metamorphics, and magmatic rocks are related tectonically, and different tectonic units are divided into major parts depending on geological and tectonic properties (Ketin, 1966; Adamia et al., 1977; Şengör and Yılmaz, 1981; Şengör et al., 1985; Göncüoğlu et al., 1997; Okay and Tüysüz, 1999). Moreover, eastern

* Correspondence: nmaden@gumushane.edu.tr

Turkey, which is known as a geologically complex domain of tectonic units, notably the Eastern Pontides, is situated along the Alp–Himalayan mountain belt (Figure 1a). In the Eastern Pontides, which are well known as one of the best protected island arc examples (Akın, 1978; Şengör and Yılmaz, 1981; Akıncı, 1984; Okay and Şahintürk, 1997), there are several plutonic rocks with different composition, size, and age range over Permo-Carboniferous to Eocene (Karslı et al., 2007; Topuz et al., 2010; Dokuz, 2011; Kaygusuz and Öztürk, 2015; Maden and Akaryalı, 2015a; Kaygusuz et al., 2016; Eyüboğlu et al., 2017; Sipahi et al., 2017; Figure 1b).

The Eastern Pontides have been defined by dividing into three subtectonic units as Northern and Southern (Özsayar et al., 1981; Güven, 1993) and axial zones (Bektaş et al., 1995; Eyüboğlu et al., 2006) on significant differences, especially in Upper Cretaceous. In the southern zone, pre-Upper Cretaceous sedimentary sequences, pre-Liassic mafic and ultramafic cumulates, and metamorphic–granitic rocks are commonly observed, whilst the northern zone is represented by the plutonic and volcanic rocks (Eyüboğlu et al., 2006). According to Eyüboğlu et al. (2010), Middle to Upper Cretaceous olistostromal mélange and upper mantle peridotites

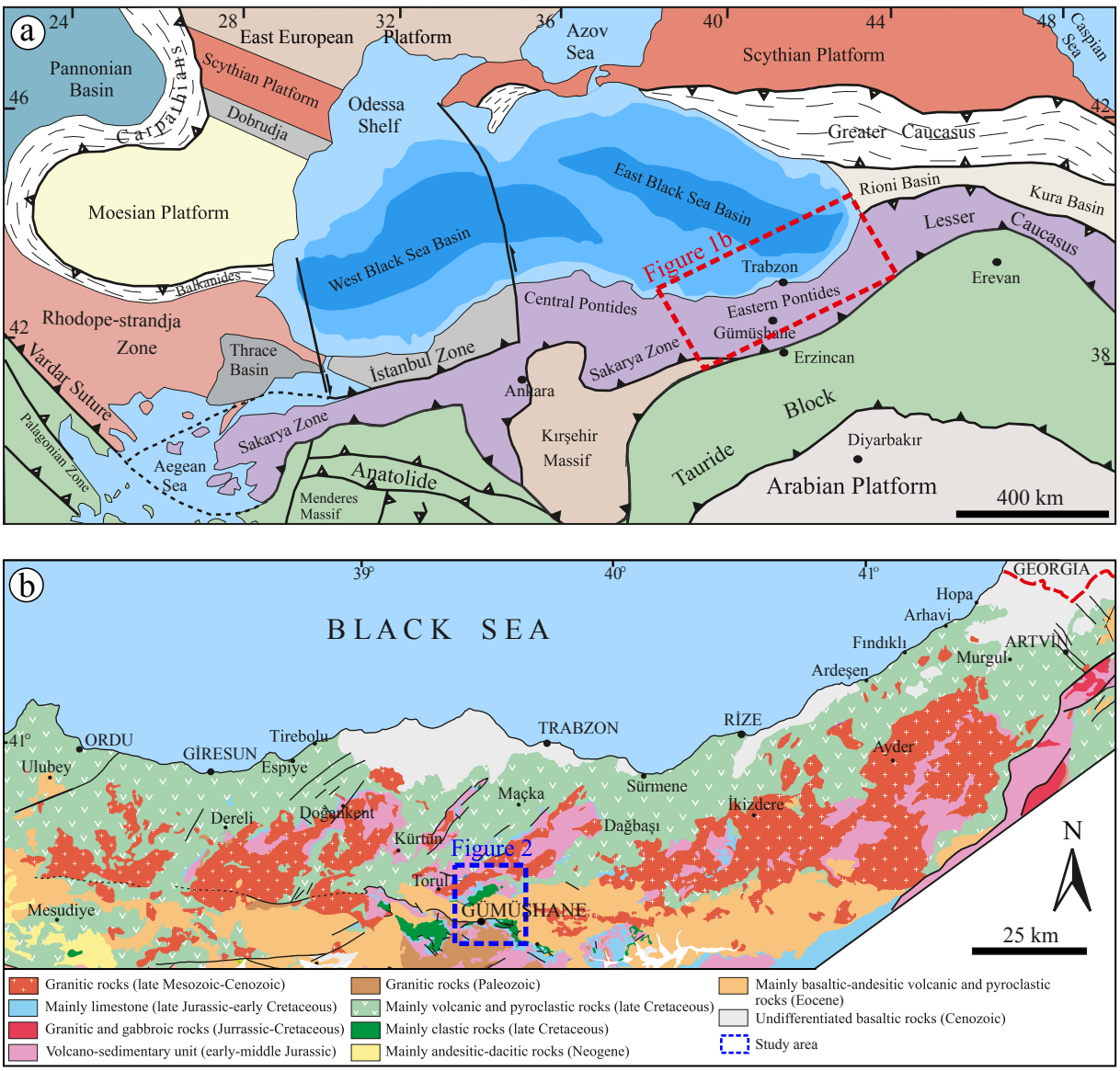

Figure 1. (a) Map of the main tectonic units of Turkey (modified after Okay and Tüysüz, 1999). (b) The geological map of the northern part of the Eastern Pontides after Eyüboğlu et al. (2014).

prevail considerably much of the axial zone. The study and sampling areas are located in the southern zone of the Eastern Pontides (NE, Turkey). The amphibolite-facies Kurtoğlu metamorphites, which consist of gneiss, schist, phyllite, and amphibolite, are basement rocks (Topuz et al., 2007; Figure 2). The basement metamorphic rocks intruded by intrusive rocks during the Carboniferous period represented by Gümüşhane and Köse granitic rocks (Topuz et al., 2010; Dokuz, 2011). The Gümüşhane Granite overlay unconformably by the Jurassic-aged volcanic and volcanoclastic assemblage (Şenköy Formation) developed during rifting of the continental margins (Kandemir and Yılmaz, 2009), and composed of felsic and granodiorite rocks (rhyolite, dacite, and microgranite). The granodiorite and granite are generally seen in the center and northern part of the region that consists predominantly of biotite, plagioclase, hornblende, K-feldspar with accessory magnetite, apatite, and zircon, whereas the felsic rocks that contain lots of feldspar and quartz are observed in the south and southeastern part of the basement. The Upper Jurassic to Lower Cretaceous limestones (Berdiga Formation) lie conformably over the volcanic and volcanoclastic rocks in the region (Pelin, 1977; Okay and Şahintürk, 1997). The carbonate rocks are conformably overlain by Late Cretaceous units consisting of sedimentary units in the southern zone (Kermutdere Formation). This means that the Upper Cretaceous, primarily indicated by volcanic rocks in the northern zone, progressed with turbiditic facies in the southern zone (Eker and Korkmaz, 2011). The Eocene basic and intermediate volcano sediments are prevalent in the study area (Alibaba Formation) and discordantly overlie the older rocks. This formation is composed of basaltic to andesitic rocks and their pyroclastics with sediments, and coal interbedded in various location.

3. Materials and methods

3.1. Gamma ray spectrometric analysis

Total surface area of Gümüşhane has 6575 km^2. The population of Gümüşhane was almost 162,748 in 2018. Gümüşhane has a population density of 25 people per square kilometer. Average life expectancy at birth in 2018 rose above 79.0 years in Gümüşhane (TURKSTAT, 2018). In the present study, in situ gamma ray survey has been performed at 162 sites (Figure 3) throughout the highest population density regions of Gümüşhane Province.

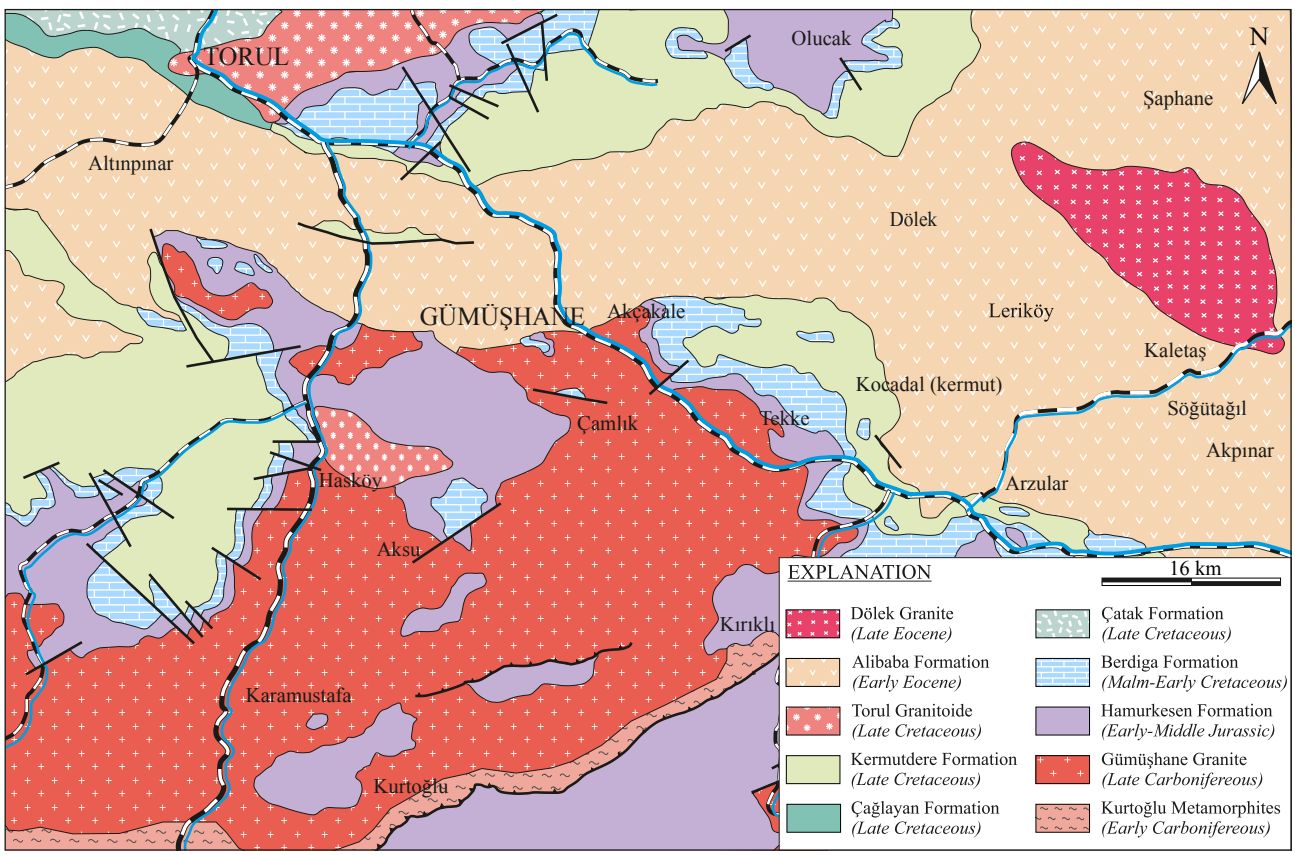

Figure 2. Geological map of the study area (modified after Güven, 1993).

The ^{238}U, ^{232}Th, and ^{40}K radionuclide concentrations could be identified with the powerful in situ gamma-ray spectrometry technique measuring radionuclides in the study region. The 512-channel, three-window gamma-survey instrument was used to detect the natural radionuclides concentrations of ^{238}U, ^{232}Th, and ^{40}K. The principal energies of g-ray from lower to higher are 1460 keV for potassium, 1760 keV for uranium, and 2620 keV for thorium. The ^{40}K activity concentration measurements were determined directly from the 1460 keV emissions. The ^{232}Th and ^{238}U activities during the survey were identified from daughter product ^{208}Tl and ^{214}Bi, respectively (IAEA, 2003; Ray et al., 2008).

The NaI(Tl) scintillation detector, housing the sensor, was mounted directly on the fresh outcrops with flat areas. Throughout the survey, it was guaranteed that the 2π geometry was used for in situ measurements. During the measurements, it was kept away from the environmental effects that could cause erroneous reading. The measurement precision and radiation strength determine the measurement time. An ideal measurement time was verified experimentally to ensure accurate results. If the spectrometry detector of 2 × 2 inches NaI(Tl) is operated and the counting time is set to 180 s, the concentration results will have the order of 0.1% for K, 1 ppm for U and Th. The counting time shorter than 3 min leads to smaller stability of obtained results (IAEA, 2003; Maden and Akaryalı, 2015b; Maden et al., 2019).

In this study, 162 measurements were carried out at the stations shown in Figure 3; they were from granite (n = 113), andesite/basalt (n = 15), microgranite (n = 11), metagranite (n = 9), sandstone (n = 6), and with very few on diorite-diabase-diorite porphyry, granodiorite, micaschist, conglomerate in the study region. The measurement points were selected among the fresh outcrops through the highway near the residential area. The distances between the survey locations are variable and irregular due to the topographical condition of the region.

3.2. Radiological hazard indices

The participation to absorbed dose rate (D_{abs}) in the air due to radionuclides is related to the concentrations of ^{238}U, ^{232}Th, and ^{40}K in the rocks and soil. Beck (1972) showed the probability of linear relationship between the terrestrial gamma radiation and radionuclide concentrations of ^{238}U, ^{232}Th, and ^{40}K in soil and rocks. The outdoor and indoor absorbed dose rates (D_{out}, D_{in}) could be determined using the equations suggested by UNSCEAR (2000).

$$D_{out}(nGy\ h^{-1}) = 0.462C_U + 0.604C_{Th} + 0.0417C_K \quad (1)$$

$$D_{in}(nGy\ h^{-1}) = 0.92C_U + 1.1C_{Th} + 0.081C_K \quad (2)$$

where C_U, C_{Th}, and C_K are the concentrations of ^{238}U, ^{232}Th, and ^{40}K in Bq kg^{-1}, respectively.

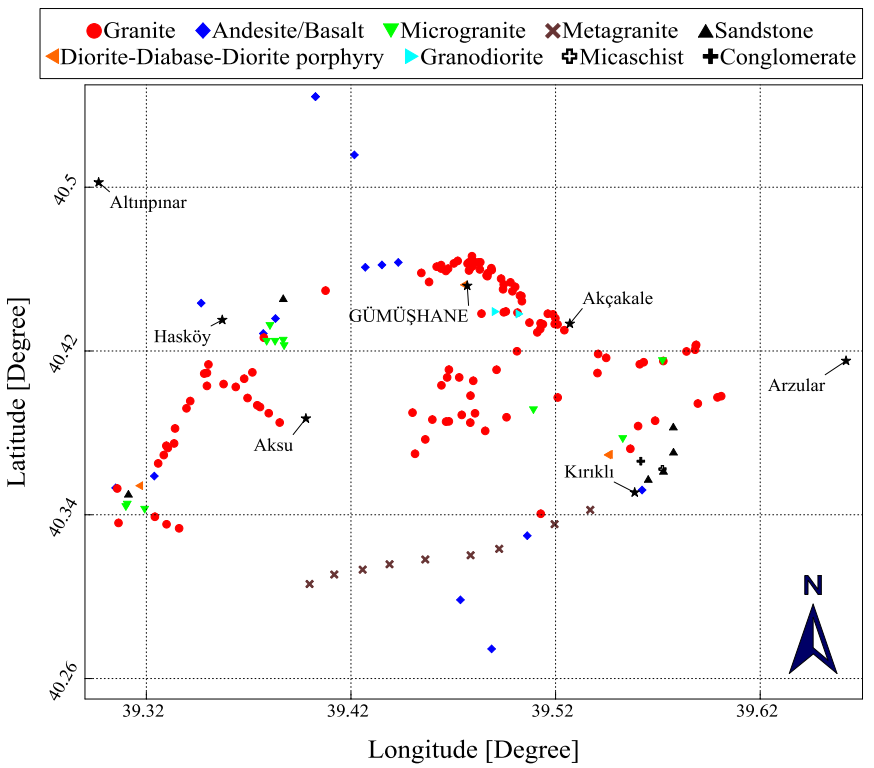

Figure 3. The radioelemental survey locations gathered from Gümüşhane province. The coloured symbols demonstrate the lithology of the survey locations.

The external hazard index (H_{ex}) due to the emitted gamma rays and internal hazard index (H_{in}) due to the radon and its short-lived products were proposed in equations 3 and 4.

$$H_{ex} = \frac{C_u}{370} + \frac{C_{Th}}{259} + \frac{C_K}{4810} \leq 1 \quad (3)$$

$$H_{in} = \frac{C_u}{185} + \frac{C_{Th}}{259} + \frac{C_K}{4810} \leq 1 \quad (4)$$

where C_U, C_{Th}, and C_K are the concentrations of ^{238}U, ^{232}Th, and ^{40}K in Bq kg^{-1}, respectively. The H_{ex} and H_{in} values must be less than 1.

The absorbed dose to effective dose conversion coefficient (0.7 Sv Gy^{-1}) and the outdoor occupancy factor (0.2) proposed by UNSCEAR (2000) were employed to calculate the AEDE values. Outdoor, indoor, and total annual effective dose equivalent ($AEDE_{out}$, $AEDE_{in}$, and $AEDE_{tot}$) values can be identified by subsequent equivalences (UNSCEAR, 2000; Tzortzis et al., 2003):

$$AEDE_{out}(mSv\ yr^{-1}) = D_{out}(nGy\ h^{-1}) \times 8760h \times 0.2 \times 0.7 \times 10^{-3} \quad (5)$$

$$AEDE_{in}(mSv\ yr^{-1}) = D_{in}(nGy\ h^{-1}) \times 8760h \times 0.8 \times 0.7 \times 10^{-3} \quad (6)$$

$$AEDE_{tot}(mSv\ yr^{-1}) = AEDE_{in} + AEDE_{out} \quad (7)$$

where D_{out} and D_{in} are the outdoor and indoor air absorbed dose rate values. ELCR is outlined as the likelihood that people will contract cancer if subjected to a certain radiation dose ranges during their lifetime. The life-long cancer risk was computed by the following equation (ICRP, 1990; Taşkın et al., 2009).

$$ELCR_{out} = AEDE_{out} \times DL \times RF \quad (8)$$

$$ELCR_{in} = AEDE_{in} \times DL \times RF \quad (9)$$

$$ELCR_{tot} = ELCR_{in} + ELCR_{out} \quad (10)$$

where $AEDE_{out}$, $AEDE_{in}$, $AEDE_{tot}$ are outdoor, indoor, and total AEDE values in mSv yr^{-1}; $ELCR_{out}$, $ELCR_{in}$, and $ELCR_{tot}$ are outdoor, indoor, and total ELCR; *DL* is the average life span of human (60 years) and RF is fatal risk factor (5.10^{-2} Sv^{-1}). The International Commission on Radiological Protection (ICRP) defined the RF values of 0.05 for the public in the case of stochastic effects (ICRP, 1990).

4. Results and discussions

The gathered natural radionuclide concentration values of ^{238}U, ^{232}Th, and ^{40}K whose survey locations are given in Figure 3 change greatly based on the lithology and geochemistry of rocks within the study area (Table 1; Figures 4a, 4c, and 4e). In Gümüşhane Province, the concentration of ^{238}U changes from 2.5 to 227.1 Bq kg^{-1}, that of ^{232}Th varies from 3.3 to 193.2 Bq kg^{-1}, and that of ^{40}K ranges from 62.6 to 1940.6 Bq kg^{-1}. The average values of ^{238}U, ^{232}Th, and ^{40}K given in Table 1 were measured to be 58.7 ± 34.3 Bq kg^{-1}, 62.7 ± 37.2 Bq kg^{-1}, 1026.8 ± 486.0 Bq kg^{-1}, respectively. While the highest average radionuclide concentration values were obtained from the granitic rocks such as granite, microgranite, and metagranite, the lowest radionuclide concentration values were measured on the andesite/basalt units (Table 1). The mean values of ^{238}U, ^{232}Th and ^{40}K are 59.9 ± 35.0 Bq kg^{-1}, 67.6 ± 36.3 Bq kg^{-1}, 1086.6 ± 462.6 Bq kg^{-1}, for granites; 88.0 ± 28.9 Bq kg^{-1}, 97.9 ± 40.8 Bq kg^{-1}, 1356.1 ± 449.7 Bq kg^{-1} for microgranites; 77.0 ± 36.0 Bq kg^{-1}, 52.2 ± 16.9 Bq kg^{-1}, 1230.4 ± 226.9 Bq kg^{-1} for metagranites and 41.8 ± 14.3 Bq kg^{-1}, 34.8 ± 23.2 Bq kg^{-1}, 484.1 ± 260.8 Bq kg^{-1} for andesite/basalt, respectively. The frequency distributions of ^{238}U, ^{232}Th and ^{40}K concentration values are given in Figures 4b, 4d, and 4f. The numerical results represent that the mean ^{238}U, ^{232}Th, and ^{40}K radionuclide values for granitic rocks are greater than the worldwide average value (40 Bq kg^{-1} for ^{238}U and ^{232}Th, 580 Bq kg^{-1} for ^{40}K) of natural radionuclide concentrations in Gümüşhane Province (UNSCEAR, 2000). Since the greater part of measurements has granitic composition, a number of the measurements are closer to the K-apex in the triangular U-Th-K ternary plot (Figure 5). The radionuclide activity concentration range in the study area could be the reason of the K-bearing mineral proportion within the rocks. High amounts of radioactive elements are related to the radioactive accessory mineral ensemble of igneous rocks of monazite, apatite, titanite, and zircon (Pagel, 1982).

The maps of D_{out} and D_{in} values and frequency distribution plots are given in Figure 6. The computed D_{out} and D_{in} values were found to be in the range of 12.3–261.5 nGy h^{-1} and 23.4–497.0 nGy h^{-1} with a mean value of 107.8 ± 51.5 nGy h^{-1} and 206.2 ± 98.1 nGy h^{-1}, respectively (Figures 6b and 6d). Mean lowest D_{out} and D_{in} values were computed for the dioritic rocks, and mean highest D_{out} and D_{in} values were determined from the granitic rocks and andesite/basalt units. The average D_{out} and D_{in} values are 113.8 ± 50.1 and 217.4 ± 95.5 nGy h^{-1} for granites, 156.3 ± 51.9 and 298.5 ± 98.6 nGy h^{-1} for microgranites, 118.4 ± 24.5 and 228 ± 47.9 nGy h^{-1} for metagranites, and 60.5 ± 24.0 and 115.9 ± 45.3 nGy h^{-1} for andesite/basalts, respectively. In the granitic rocks, the average D_{out} and D_{in} values are 1.7 and 2.3 times higher than the worldwide outdoor and indoor values (59 nGy h^{-1} and 84 nGy h^{-1}) given in the UNSCEAR (2000) report. The maximum D_{out} and D_{in} values are seen in the middle of the study region outside the city center where the granitoid units are exposed (Figures 6a and 6c). There is an important relationship between the radiation stages and the mineral amounts (feldspar, orthoclase, etc.) of the Gümüşhane Granitoid.

The estimated H_{ex} and H_{in} values and frequency distributions plots are given in Figure 7. The computed H_{ex} and H_{in} values extended from 0.07 to 1.52 and 0.08 to

Table 1. The ^{238}U, ^{232}Th, and ^{40}K (Bq kg^{-1}) activity concentrations, outdoor and indoor air absorbed dose rates (D_{out}, D_{in}), and external and internal hazard index (H_{ex}, H_{in}) values in the study region.

Rock Type	Formation	N	K [Bq kg^{-1}]		U [Bq kg^{-1}]		Th [Bq kg^{-1}]		D_{out} [nGy h^{-1}]		D_{in} [nGy h^{-1}]		H_{ex}		H_{in}	
			Range	Mean ± σ	Range	Mean ± σ	Range	Mean ± σ	Range	Mean ± σ	Range	Mean ± σ	Range	Mean ± σ	Range	Mean ± σ
Granite	Gümüşhane Granitoid	113	72–1790.4	1086.6 ± 462.6	2.5–227.1	59.9 ± 35	3.3–161.8	67.6 ± 36.3	12.3–223.1	113.8 ± 50.1	23.4–430.6	217.4 ± 95.5	0.07–1.29	0.65 ± 0.29	0.08–1.91	0.81 ±0.37
Andesite/ Basalt	Alibaba Formation	15	62.6–1017.3	484.1 ± 260.8	18.8–65	41.8 ± 14.3	6.5–75.3	34.8 ± 23.2	28–99.7	60.5 ± 24	54.6–189.5	115.9 ± 45.3	0.16–0.59	0.35 ± 0.14	0.25–0.75	0.46 ±0.17
Microgranite	Gümüşhane Granitoid	11	710.5–1940.6	1356.1 ± 449.7	51.3–141.7	88 ± 28.9	51–193.2	97.9 ± 40.8	88.1–261.5	156.3 ± 51.9	168.6–497	298.5 ± 98.6	0.5–1.52	0.9 ± 0.3	0.64–1.91	1.14 ±0.37
Metagranite	Kurtoğlu Metamorphics	9	857.6–1530.6	1230.4 ± 226.9	41.9–140.2	77 ± 36	27.8–89.4	52.2 ± 16.9	81.4–163.1	118.4 ± 24.5	157–315.8	228 ± 47.9	0.45–0.92	0.67 ± 0.14	0.57–1.3	0.87 ±0.23
Sandstone	Kermutdere Formation	6	237.9–1621.3	770 ± 475.6	15.4–48.7	32.2 ± 13.3	8–53.6	30.5 ± 15.3	31.1–91.4	65.4 ± 24.9	60.7–176.1	125.5 ± 47.7	0.18–0.5	0.36 ± 0.14	0.27–0.62	0.45 ±0.15
Diorite-Diabase-Diorite porphyry	Hamurkesen Formation	4	253.5–582.2	422.6 ± 163.5	16.5–31.5	25.4 ± 6.5	14.9–20.5	17.9 ± 2.3	35.5–48.6	40.2 ± 5.8	68.1–93.8	77.3 ± 11.3	0.2–0.27	0.23 ± 0.03	0.26–0.35	0.29 ±0.04
Granodiorite	Gümüşhane Granitoid	2	472.6–763.7	618.2 ± 205.8	16.3–65.3	40.8 ± 34.7	11.1–71.5	41.3 ± 42.7	34–105.2	69.6 ± 50.4	65.5–200.6	133.1 ± 95.5	0.19–0.61	0.4 ± 0.3	0.23–0.79	0.51 ±0.4
Micaschist	Kurtoğlu Metamorphics	1	1921.8	1921.8	66.7	66.7	70.6	70.6	153.6	153.6	294.7	294.7	0.85	0.85	1.03	1.03
Conglomerate	Hamurkesen Formation	1	832.6	832.6	21.6	21.6	38.3	38.3	67.8	67.8	129.4	129.4	0.38	0.38	0.44	0.44
All data		162	62.6–1940.6	1026.8 ± 486	2.5 ± 227.1	58.7 ± 34.3	3.3 ± 193.2	62.7 ± 37.2	12.3 ± 261.5	107.8 ± 51.5	23.4 ± 497	206.2 ± 98.1	0.07 ± 1.52	0.61 ± 0.3	0.08 ± 1.91	0.77 ± 0.37
World average				580[a]		40[a]		40[a]		59[a]		84[a]		1[a]		1[a]

[a]UNSCEAR (2000)

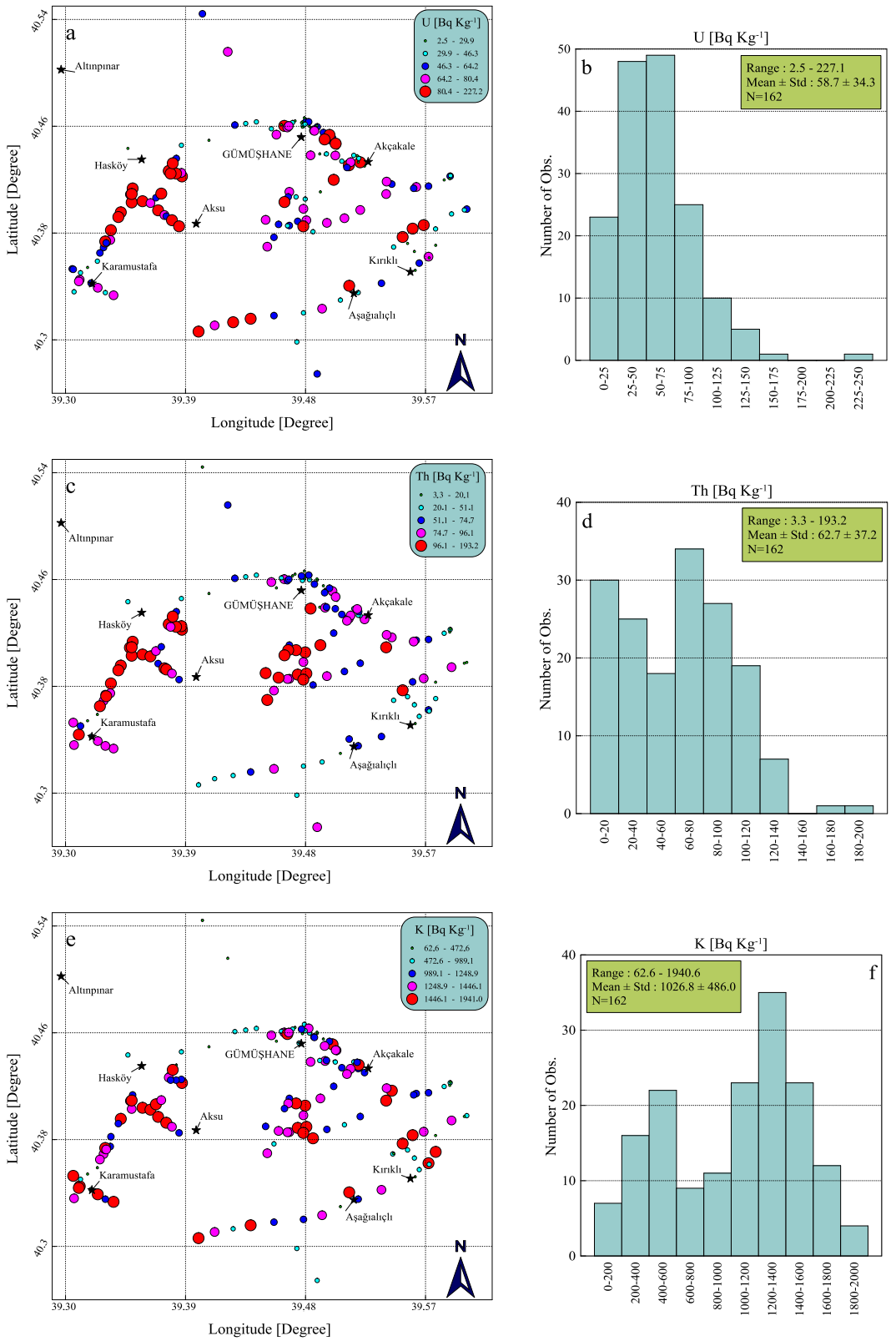

Figure 4. The distribution of specific activity concentrations for 162 in situ measurements in the Gümüşhane Granitoid. The distribution map of the measured specific activities of ^{238}U, (a), ^{232}Th (c), and ^{40}K (e). Frequency distribution of activity concentrations of ^{238}U (b), ^{232}Th (d), and ^{40}K (f) of the Gümüşhane Granitoid.

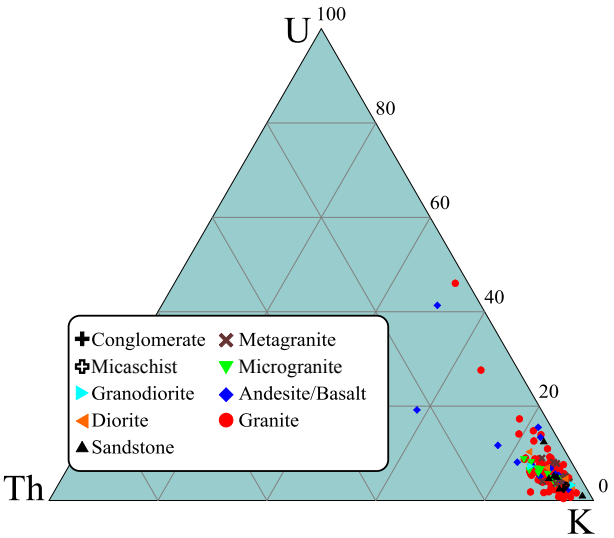

Figure 5. Plots of K–U–Th ternary diagram showing the concentrations of ^{40}K, ^{238}U, and ^{232}Th in Gümüşhane Province.

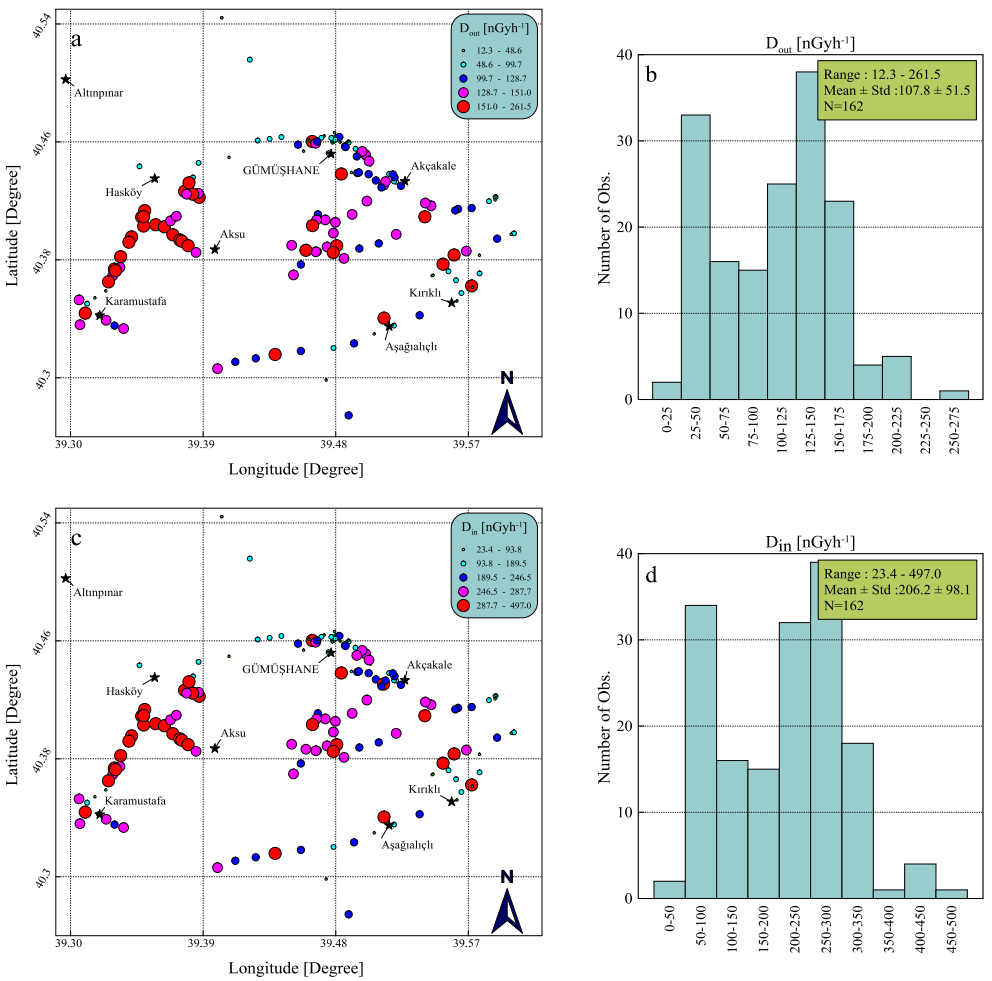

Figure 6. The map of the outdoor (a) and indoor (c) absorbed dose rate distribution for 162 in situ measurements in the study region. The histogram distributions of outdoor (b) and indoor (d) absorbed dose rate values for the Gümüşhane Granitoid.

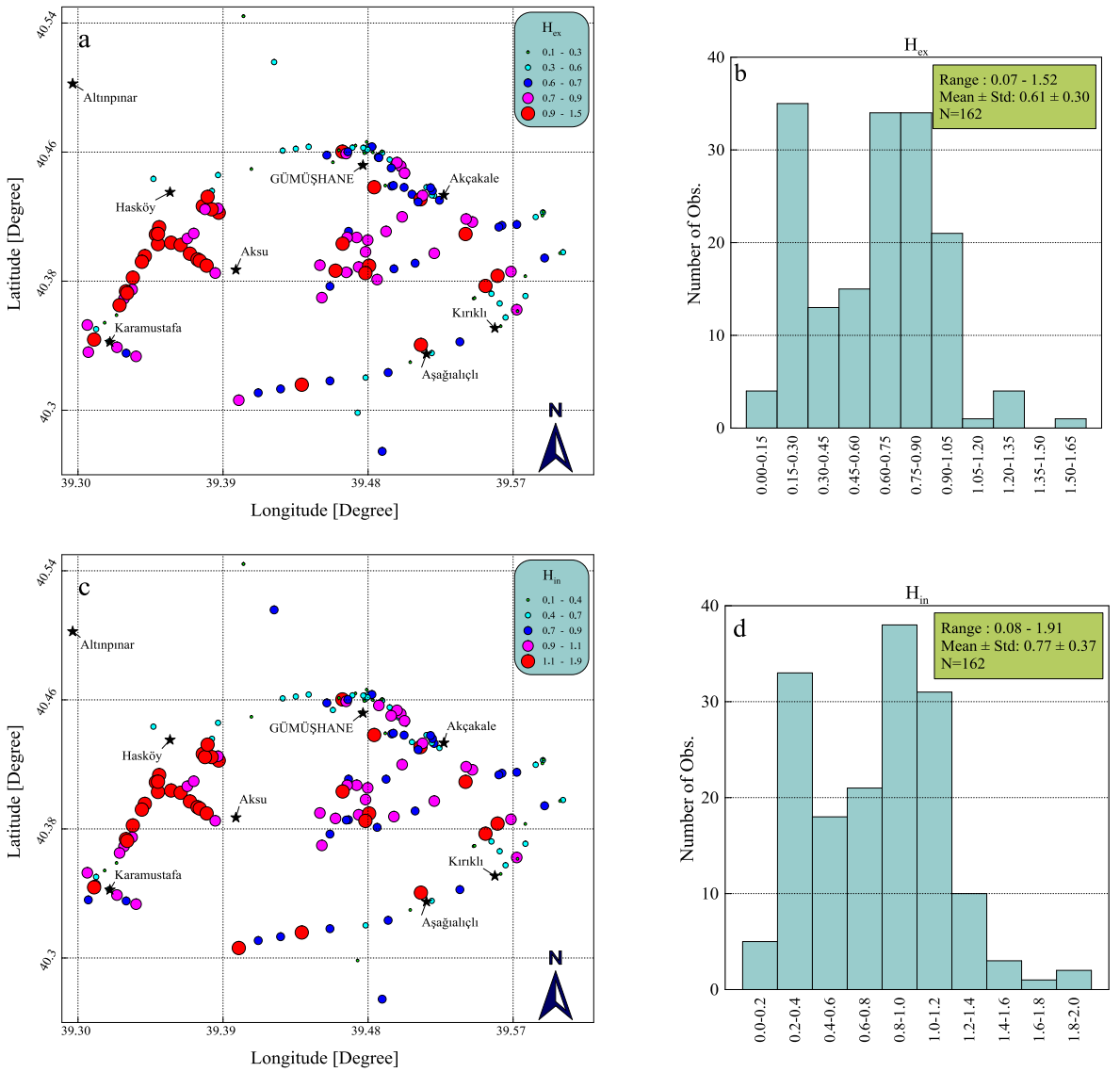

Figure 7. The map of the external hazard index (a) and internal hazard index (c) values for 162 in situ measurements in the study region. The histogram distributions of external hazard index (b) and internal hazard index (d) values for the Gümüşhane Granitoid.

1.91. The average H_{ex} and H_{in} values are obtained as 0.61 ± 0.30 and 0.77 ± 0.37, respectively, which is less than the recommended permissible value of 1 by UNSCEAR (2000) report. The computed mean H_{in} values for microgranites are higher than that of the world mean values of 1 recommended by UNSCEAR (2000) listed in Table 1.

The $AEDE_{out}$, $AEDE_{in}$, and $AEDE_{tot}$ values in the study region presented in Table 2 and Figure 8 were determined to be in the range of 15.1–320.7 mSv yr^{-1}, 114.7–2437.9 mSv yr^{-1} and 129.9–2758.6 mSv yr^{-1}, respectively. The mean value was determined to be 132.2 ± 63.2 mSv yr^{-1}, 1011.3 ± 481.4 mSv yr^{-1} and 1143.6 ± 544.6 mSv yr^{-1} for the $AEDE_{out}$, $AEDE_{in}$, and $AEDE_{tot}$, respectively. The computed $AEDE_{out}$, $AEDE_{in}$, and $AEDE_{tot}$ values for granite, metagranite, microgranite, and andesite/basalt are higher than the world mean value, as suggested by UNSCEAR (2000) given in Figures 8a, 8c, and 8d and Table 2. The ICRP notifies AEDE of 1 and 20 mSv yr^{-1} for the human being and the medical staff, respectively (ICRP, 1993). The world mean AEDE from outdoor terrestrial gamma radiation is 70 mSv yr^{-1} (UNSCEAR, 1988). Thus, the calculated $AEDE_{out}$ values are greater than the world mean value but smaller than that of Isparta (Kalyoncuoğlu et al., 2015), Çanakkale (Örgün et al., 2007), Artvin (Kobya et al., 2015), and Kırklareli (Taşkın et al., 2009) listed in Table 3.

Table 2. The external and internal hazard index (H_{ex}, H_{in}) values; the outdoor, indoor, and total annual effective dose equivalents ($AEDE_{out}$, $AEDE_{in}$, $AEDE_{tot}$); outdoor ($ELCR_{out}$), indoor ($ELCR_{in}$), and total ($ELCR_{tot}$) excess lifetime cancer risk for the study region.

Rock Type	Formation	N	$AEDE_{out}$ [mSv yr^{-1}]		$AEDE_{in}$ [mSv yr^{-1}]		$AEDE_{tot}$ [mSv yr^{-1}]		$ELCR_{out}$ [10^{-3}]		$ELCR_{in}$ [10^{-3}]		$ELCR_{tot}$ [10^{-3}]	
			Range	Mean ± σ	Range	Mean ± σ	Range	Mean ± σ	Range	Mean ± σ	Range	Mean ± σ	Range	Mean ± σ
Granite	Gümüşhane Granitoid	113	15.1–273.6	139.6 ± 61.5	114.7–2112.6	1066.7 ± 468.3	129.9–2386.2	1206.3 ± 529.8	0.05–0.82	0.42 ± 0.18	0.34–6.34	3.20 ± 1.41	0.39–7.16	3.62 ±1.59
Andesite/ Basalt	Alibaba Formation	15	34.4–122.2	74.2 ± 29.5	268.1–929.5	568.5 ± 222.3	302.5–1051.7	642.7 ± 251.7	0.10–0.37	0.22 ± 0.09	0.8–2.79	1.71 ± 0.67	0.91–3.16	1.93 ±0.76
Microgranite	Gümüşhane Granitoid	11	108.1–320.7	191.7 ± 63.7	827.1–2437.9	1464.1 ± 483.5	935.2–2758.6	1655.8 ± 547.2	0.32–0.96	0.58 ± 0.19	2.48–7.31	4.39 ± 1.45	2.81–8.28	4.97 ±1.64
Metagranite	Kurtoğlu Metamorphics	9	99.8–200	145.3 ± 30	770.2–1549	1118.4 ± 235.1	870.0–1749.1	1263.7 ± 265.2	0.30–0.60	0.44 ± 0.09	2.31–4.65	3.36 ± 0.71	2.61–5.25	3.79 ±0.8
Sandstone	Kermutdere Formation	6	38.2–112.1	80.2 ± 30.5	297.6–863.8	615.9 ± 233.8	335.8–975.9	696.1 ± 264.3	0.11–0.34	0.24 ± 0.09	0.89–2.59	1.85 ± 0.7	1.01–2.93	2.09 ±0.79
Diorite-Diabase-Diorite porphyry	Hamurkesen Formation	4	43.5–59.6	49.3 ± 7.1	334.2–459.9	379.4 ± 55.7	377.7–519.5	428.7 ± 62.8	0.13–0.18	0.15 ± 0.02	1.00–1.38	1.14 ± 0.17	1.13–1.56	1.29 ±0.19
Granodiorite	Gümüşhane Granitoid	2	41.6–129	85.3 ± 61.8	321.4–984.1	652.8 ± 468.6	363.1–1113.2	738.1 ± 530.4	0.12–0.39	0.26 ± 0.19	0.96–2.95	1.96 ± 1.41	1.09–3.34	2.21 ±1.59
Micaschist	Kurtoğlu Metamorphics	1	188.4	188.4	1445.8	1445.8	1634.2	1634.2	0.57	0.57	4.34	4.34	4.90	4.90
Conglomerate	Hamurkesen Formation	1	83.2	83.2	635	635	718.1	718.1	0.25	0.25	1.90	1.90	2.15	2.15
All data		162	15.1–320.7	132.2 ± 63.2	114.7–2437.9	1011.3 ± 481.4	129.9–2758.6	1143.6 ± 544.6	0.05–0.96	0.40 ± 0.19	0.34–7.31	3.03 ± 1.44	0.39–8.28	3.43 ± 1.63
World average				70[a]		460[b]		520[c]		0.29[b]		1.16[b]		1.45[b]

[a]UNSCEAR (2000), [b]UNSCEAR (1993), [c]Taşkın et al. (2009)

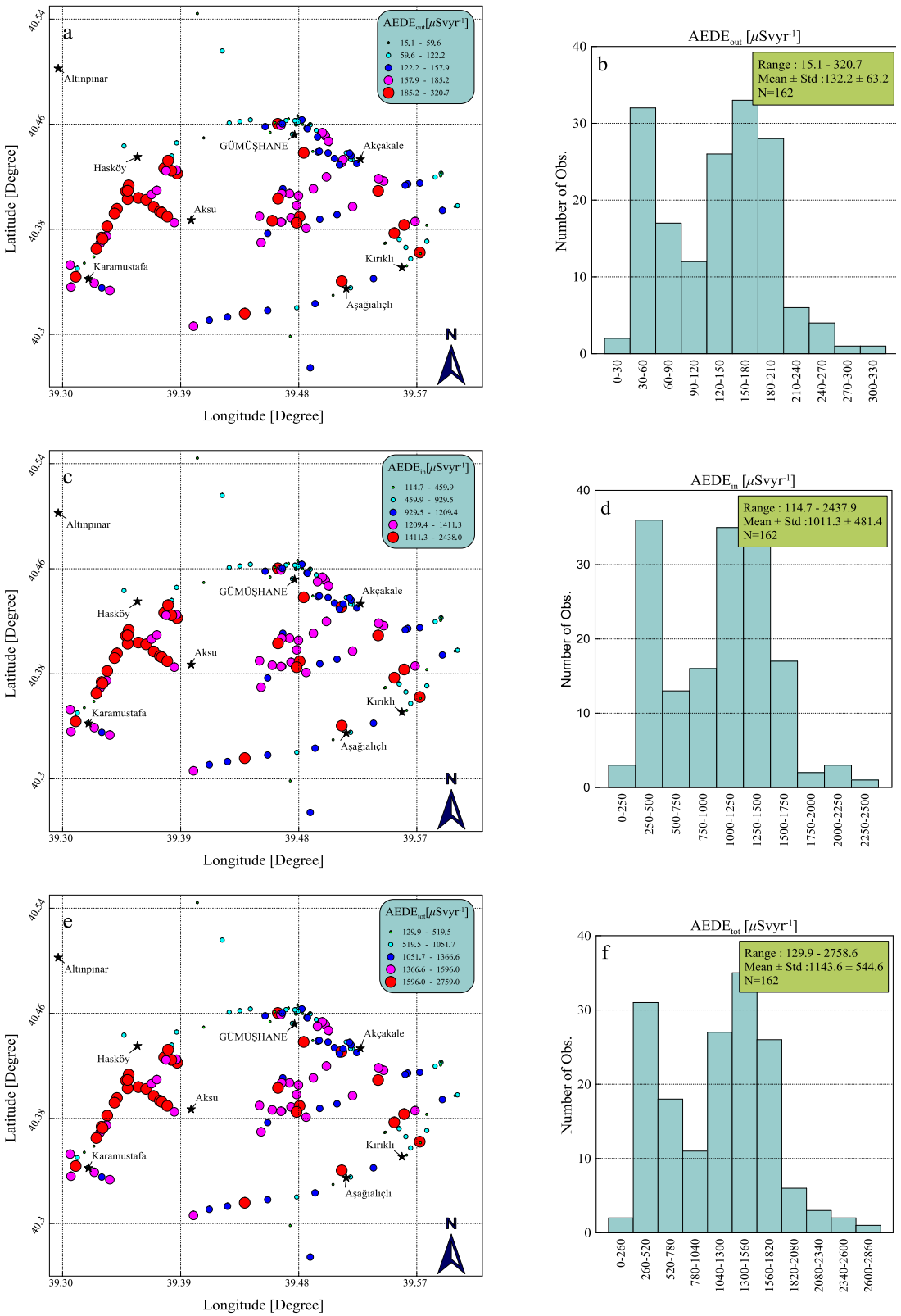

Figure 8. The distributions of outdoor (a), indoor (c), and total (e) annual effective dose equivalent values for the study region. Frequency distributions of outdoor (b), indoor (d), and total (f) annual effective dose equivalent values of the Gümüşhane Granitoid.

Table 3. Comparison of annual effective dose equivalent and excess lifetime cancer risk values with previous studies.

References	Area	Annual effective dose equivalent [mSv yr^{-1}]	Excess lifetime cancer risk [10^{-3}]
Karahan and Bayülke (2000)	İstanbul (Turkey)	80	
Bozkurt et al. (2007)	Şanlıurfa (Turkey)	74.7	
Örgün et al. (2007)	Çanakkale (Turkey)	260	
Kam and Bozkurt (2007)	Kastamonu (Turkey)	67	
Değerlier et al. (2008)	Adana (Turkey)	82	
Taşkın et al. (2009)	Kırklareli (Turkey)	144	0.51
Kapdan et al. (2011)	Yalova (Turkey)	103.38	0.42
Kalyoncuoğlu et al. (2015)	Isparta (Turkey)	429.53	1.5
Kobya et al. (2015)	Artvin (Turkey)	214.5	0.75
Kapdan et al. (2018)	Ankara (Turkey)	71.8	0.27
This study	Gümüşhane (Turkey)	132.2	0.40
UNSCEAR (2000)	World	70	0.29

The average $ELCR_{out}$, $ELCR_{in}$, and $ELCR_{tot}$ values for Gümüşhane Province given in Figure 9 are calculated to be $0.40 \pm 0.19 \times 10^{-3}$, $3.03 \pm 1.44 \times 10^{-3}$, and $3.43 \pm 1.63 \times 10^{-3}$, which are higher than the world's mean $ELCR_{out}$, $ELCR_{in}$, and $ELCR_{tot}$ values of 0.29×10^{-3}, 1.16×10^{-3}, and 1.45×10^{-3} (UNSCEAR, 2000). The ELCR values shown in Figures 9b, 9d, and 9f varied from 0.05 to 0.96, 0.34 to 7.31, and 0.39 to 8.28. The mean values of cancer risk factor for the investigated regions surpass the limit level given in the UNSCEAR (2000) report. In this study, life expectancy at birth for Gümüşhane Province was given as 79.8 years (TURKSTAT, 2018). This result obtained for ELCR represents the risk of contracting cancer for people who will spend most of their lifespan in the studied regions.

5. Conclusion

The measurements have been carried out in Gümüşhane Province using gamma-ray spectrometry equipment. The following results are derived from the current study:

1. The mean value of radionuclide contents for ^{238}U, ^{232}Th, and ^{40}K revealed to be 58.7 Bq kg^{-1}, 62.7 Bq kg^{-1}, and 1026.8 Bq kg^{-1}, which are greater than the world's mean value of 40 Bq kg^{-1} (for ^{238}U and ^{232}Th) and 580 Bq kg^{-1} (for ^{40}K).

2. The highest natural radiation areas demonstrated in Figure 4 are associated with the K-rich minerals (Biotite and K-feldspars) and accessories (apatite, zircon, allanite, titanite, and monazite) which are mainly present in granitic rocks.

3. The H_{in} and H_{ex} values varied from 0.08 to 1.91 and from 0.07 to 1.52, respectively.

4. The average outdoor AEDE and outdoor ELCR values for Gümüşhane Province were 132.2 ± 63.2 mSv yr^{-1} and $0.40 \pm 0.19 \times 10^{-3}$, respectively.

5. Numerical results indicate that the AEDE and ELCR values were fairly greater in Gümüşhane Province than the world's mean value. There would be a radiation hazard for people inhabiting in Gümüşhane.

6. It was observed that the region with the highest values in the radiological hazard maps (Figures 8 and 9) was quite compatible with the regions having granitic rocks such as granite, metagranite, microgranite, and granodiorite.

Acknowledgment

This study has been supported by Gümüşhane University, Scientific Research Projects Coordination Department. Project Number: 2012.02.1717.3. We would like to thank anonymous reviewers for their critical comments and suggestions, which improved the quality of the paper. We are also grateful to the editorial handling of Alper Baba and Orhan Tatar for their constructive and helpful feedback, and timely processing of the manuscript.

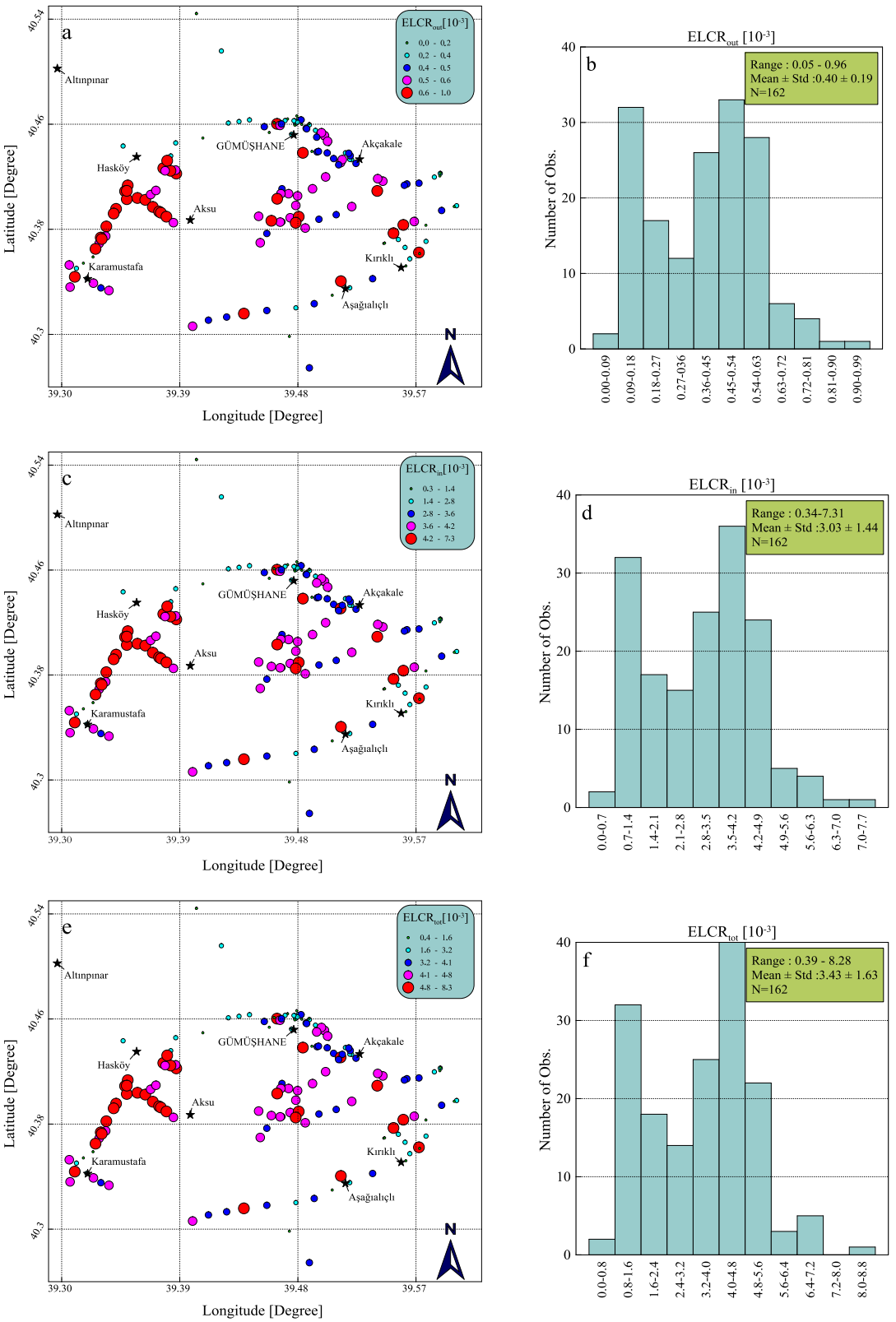

Figure 9. The distributions of outdoor (a), indoor (c), and total (e) excess lifetime cancer risk for Gümüşhane Province. Frequency distributions of outdoor (b), indoor (d), and total (f) excess lifetime cancer risks of the study region.

References

Adamia SA, Lordkipanidze MB, Zakariadze GS (1977). Evolution of an active continental margin as exemplified by the Alpine history of the Caucasus. Tectonophysics 40: 183-189.

Akın H (1978). Geologie, Magmatismus und Lagerstaettenbildung in ostpontischen Gebirge-Turkei aus der Sicht der Plattentektonik. Geologische Rundschau 68: 253-283 (in German).

Akıncı ÖT (1984). The Eastern Pontide volcano-sedimentary belt and associated massive sulphide deposits. In: Dixon JE, Robertson AHF (editors). The Geological Evolution of the Eastern Mediterranean: Geological Society Special Publication 17: 415-428.

Beck HL (1972). The physics of environmental radiation fields. Natural radiation environment II, CONF-720805 P2. Proceedings of the Second International Symposium on the Natural Radiation Environment.

Bektaş O, Yılmaz C, Taslı K, Akdağ K, Özgür S (1995). Cretaceous rifting of the eastern Pontide carbonate platform (NE Turkey): the formation of carbonates breccias and turbidites as evidences of a drowned platform. Geologia 57 (1-2): 233-244.

Bozkurt A, Yorulmaz N, Kam E, Karahan G, Osmanlıoğlu AE (2007). Assessment of environmental radioactivity for Şanliurfa region of Southeastern Turkey. Radiation Measurements 42 (8): 1387-1391.

Chen CJ, Lin YM (1996). Assessment of building materials for compliance with regulations of ROC. Environment International 22: 221-226.

Çınar H, Altundaş S, Çelik N, Maden N (2017). In situ gamma ray measurements for deciphering of radioactivity level in Sarıhan pluton area of northeastern Turkey. Arabian Journal of Geosciences 10: 435. doi: 10.1007/s12517-017-3225-4

Değerlier M, Karahan G, Ozger G (2008). Radioactivity concentrations and dose assessment for soil samples around Adana, Turkey. Journal of Environmental Radioactivity 99 (7): 1018-1025.

Dokuz A (2011). A slab detachment and delamination model for the generation of Carboniferous high-potassium I-type magmatism in the Eastern Pontides, NE Turkey: The Köse composite pluton. Gondwana Research 19 (4): 926-944.

Durusoy A, Yildirim M (2017). Determination of radioactivity concentrations in soil samples and dose assessment for Rize Province, Turkey. Journal of Radiation Research and Applied Sciences 10: 348-352.

Eker ÇS, Korkmaz S (2011). Mineralogy and whole rock geochemistry of late Cretaceous sandstones from the eastern Pontides (NE Turkey). Neues Jahrbuch für Mineralogie-Abhandlungen 188: 235-256.

Eyüboğlu Y, Bektaş O, Seren A, Maden N, Jacoby WR et al. (2006). Three axial extensional deformation and formation of the Liassic rift basins in the Eastern Pontides (NE Turkey). Geologica Carpathica 57 (5): 337-346.

Eyüboğlu Y, Dilek Y, Bozkurt E, Bektaş O, Rojay B et al. (2010). Structure and geochemistry of an Alaskan-type ultramafic–mafic complex in the Eastern Pontides, NE Turkey. Gondwana Research 18: 230-252.

Eyüboğlu Y, Santosh M, Yi K, Tüysüz N, Korkmaz S et al. (2014). The Eastern Black Sea-type volcanogenic massive sulfide deposits: geochemistry, zircon U-Pb geochronology and an overview of the geodynamics of ore genesis. Ore Geology Reviews 59: 29-54.

Göncüoğlu MC, Kozlu H, Dirik K (1997). Pre-Alpine and Alpine terranes in Turkey: explanatory notes to the terrane map of Turkey. Annales Géologiques des Pays Helleniques 37: 515-536.

Güven İH (1993). Doğu Karadeniz Bölgesi'nin 1/250000 ölçekli jeolojik ve metalojenik haritası, MTA, Ankara (in Turkish).

IAEA (2003). Guidelines for Radioelement Mapping Using Gamma Ray Spectrometry Data. IAEA Technical Reports Series 1363, International Atomic Energy Agency, Vienna.

ICRP (1990). Recommendations of the International Commission on Radiological Protection. v21(1-3), publication 60.

ICRP (1993). Protection Against Radon-222 at Home and at Work. ICRP Publication 65. Ann. ICRP 23(2).

Kalyoncuoğlu UY (2015). In situ gamma source radioactivity measurement in Isparta plain, Turkey. Environmental Earth Sciences 73: 3159-3175.

Kam E, Bozkurt A (2007). Environmental radioactivity measurements in Kastamonu region of northernTurkey. Applied Radiation and Isotopes 65: 440-444.

Kandemir R, Yılmaz C (2009). Lithostratigraphy, facies, and deposition environment of the lower Jurassic Ammonitico Rosso type sediments (ARTS) in the Gümüşhane area, NE Turkey: implications for the opening of the northern branch of the NeoTethys Ocean. Journal of Asian Earth Sciences 34: 586-598.

Kapdan E, Altinsoy N, Karahan G, Yuksel A (2018). Outdoor radioactivity and health risk assessment for capital city Ankara, Turkey. Journal of Radioanalytical and Nuclear Chemistry 318: 1033-1042.

Kapdan E, Varinlioglu A, Karahan G (2011). Radioactivity Levels and Health Risks due to Radionuclides in the Soil of Yalova, Northwestern Turkey. International Journal of Environmental Research 5 (4): 837-846.

Karahan G, Bayülken A (2000). Assessment of gamma dose rates around Istanbul, Turkey. Journal of Environmental Radioactivity 47: 213-221.

Karakelle B, Öztürk N, Köse A, Varinlioglu A, Erkol AY et al. (2002). Natural radioactivity in soil samples of Kocaeli Basin, Turkey. Journal of Radioanalytical and Nuclear Chemistry 254 (3): 649-651.

Karslı O, Chen B, Aydın F, Şen C (2007). Geochemical and Sr-Nd-Pb isotopic compositions of the Eocene Dölek and Sarıçiçek Plutons, Eastern Turkey: Implications for magma interaction in the genesis of high-K calc-alkaline granitoids in a post-collision extensional setting. Lithos 98 (1-4): 67-96.

Kaygusuz A, Arslan M, Sipahi F, Temizel İ (2016). U-Pb zircon chronology and petrogenesis of carboniferous plutons in the northern part of the Eastern Pontides, NE Turkey: Constraints for Paleozoic magmatism and geodynamic evolution. Gondwana Research 39: 327-346.

Kaygusuz A, Öztürk M (2015). Geochronology, geochemistry and petrogenesis of the Eocene Bayburt intrusions, eastern Pontide, NE Turkey: Implications for lithospheric mantle and lower crustal sources inthe high-K calc-alkaline magmatism. Journal of Asian Earth Sciences 108: 97-116.

Ketin İ (1966). Anadolu'nun tektonik birlikleri. Bulletin of the Mineral Research and Exploration 66: 20-34 (in Turkish).

Kılıç O, Belivermis M, Topçuoglu S, Cotuk Y, Coskun M et al. (2008). Radioactivity concentrations and dose assessment in surface soil samples from east and south of Marmara Region, Turkey. Radiation Protection Dosimetry 128 (3): 324-330.

Kobya Y, Taşkın H, Yeşilkanat CM, Çevik U, Karahan G et al. (2015). Radioactivity survey and risk assessment study for drinking water in the Artvin Province, Turkey. Water, Air, & Soil Pollution 226: 49.

Kurnaz A, Küçükomeroğlu B, Keser R, Okumuşoğlu NT, Korkmaz F et al. (2007). Determination of radioactivity levels and hazards of soil and sediment samples in Firtina Valley (Rize, Turkey). Applied Radiation and Isotopes 65: 1281-1289.

Küçükomeroğlu B, Karadeniz A, Damla N, Yesilkanat CM, Cevik U (2016). Radiological maps in beach sands along some coastal regions of Turkey. Marine Pollution Bulletin 112: 255-264.

Maden N, Akaryalı E (2015a). A review for genesis of continental arc magmas: U, Th, K and radiogenic heat production data from the Gümüşhane Pluton in the Eastern Pontides (NE Türkiye). Tectonophysics 664: 225-243.

Maden N, Akaryalı E (2015b). Gamma ray spectrometry for recognition of hydrothermal alteration zones related to a low sulfidation epithermal gold mineralization (eastern Pontides, NE Türkiye), Journal of Applied Geophysics 122: 74-85.

Maden N, Akaryalı E, Çelik N (2019). The in situ natural radionuclide (^{238}U, ^{232}Th and ^{40}K) concentrations in Gümüşhane granitoids: implications for radiological hazard levels of Gümüşhane city, northeast Turkey. Environmental Earth Sciences 78: 330.

Merdanoğlu B, Altınsoy N (2006). Radioactivity concentrations and dose assessment for soil samples from Kestanbol Granite Area. Radiation Protection Dosimetry 121 (4): 399-405.

Okay Aİ, Sahintürk Ö (1997). Geology of the Eastern Pontides. AAPG bulletin 68: 291-311.

Okay Aİ, Tüysüz O (1999). Tethyan sutures of northern Turkey. The Mediterranean basin: Tertiary extension within the Alpine orogeny. Geological Society London Special Publications 156: 475-515.

Örgün Y, Altınsoy N, Gültekin AH, Karahan G, Çelebi N (2005). Natural radioactivity levels in granitic plutons and groundwaters in Southeast part of Eskişehir, Turkey. Applied Radiation and Isotopes 63 (2): 267-275.

Örgün Y, Altınsoy N, Şahin SY, Güngör Y, Gültekin AH et al. (2007). Natural and anthropogenic radionuclides in rocks and beach sands from Ezine region (Çanakkale), Western Anatolia, Turkey. Applied Radiation and Isotopes 65: 739-747.

Özsayar T, Gedikoglu A, Pelin S (1981). Artvin Yöresi Yastık-Lavların Yaşına İlişkin Paleontolojik Veriler. KTÜ Yerbilimleri Dergisi 1(1): 38-42 (in Turkish).

Pagel M (1982). The mineralogy and geochemistry of uranium, thorium, and rare-earth elements in two radioactive granites of the Vosges, France. Mineralogical Magazine 46 (339): 149-161.

Pavlidou S, Koroneos A, Papastefanou C, Christofides G, Stoulos S et al. (2006). Natural radioactivity of granites used as building materials. Journal of Environmental Radioactivity 89 (1): 48-60.

Pelin S (1977). Alucra (Giresun) Güneydogu yöresinin petrol olanakları bakımından jeolojik incelenmesi. KTÜ Yayınları 87, 103p, Trabzon (in Turkish).

Ray L, Roy S, Srinivasan R (2008). High radiogenic heat production in the Kerala Khondalite Block, Southern Granulite Province, India. International Journal of Earth Sciences 97: 257-267.

Sipahi F, Kaygusuz A, Eker ÇS, Vural A, Akpınar İ (2017). Late Cretaceous arc igneous activity: The Eğrikar Monzogranite example. International Geology Review 60 (3): 382-400.

Şengör AMC, Görür N, Şaroğlu F (1985). Strike-slip faulting and related basin formation in zones of tectonic escape: Turkey as a case study. In: Biddle KT, Christie-Blick N (editors). Strike-slip deformation, basin formation and sedimentation. Special publication-Society of Economic Paleontologists and Mineralogists 37: 227-264.

Şengör AMC, Yılmaz Y (1981). Tethyan evolution of Turkey: a plate tectonic approach. Tectonophysics 75: 181-241.

Taşkın H, Karavus M, Ay P, Topuzoglu A, Hidiroglu S et al. (2009). Radionuclide concentrations in soil and lifetime cancer risk due to gamma radioactivity in Kirklareli, Turkey. Journal of Environmental Radioactivity 100: 49-53.

Topuz G, Altherr R, Schwarz WH, Dokuz A, Meyer HP (2007). Variscan amphibolite-facies rocks from the Kurtoğlu metamorphic complex (Gümüşhane area, Eastern Pontides, Turkey). International Journal of Earth Sciences 96 (5): 861-873.

Topuz G, Altherr R, Wolfgang S, Schwarz WH, Zack T et al. (2010). Carboniferous high-potassium I-type granitoid magmatism in the Eastern Pontides: The Gümüşhane pluton (NE Turkey). Lithos 116: 92-110.

TURKSTAT (Turkey Statistical Institute) (2018). Main Statistics. Web site: http://www.turkstat.gov.tr/UstMenu.do?metod=temelist, February 2, 2019.

Tzortzis M, Tsertos H, Christofides S, Christodoulides G (2003). Gamma-ray measurements of naturally occurring radioactive samples from Cyprus characteristic geological rocks. Radiation Measurements 37: 221-229.

UNSCEAR (1988). Sources and Effects of Ionizing Radiation United Nations Scientific Committee on the Effect of Atomic Radiation, United Nation, New York.

UNSCEAR (1993). Sources and effects of ionizing radiation report to the general assembly with annexes United Nations, New York, pp. 73-98.

UNSCEAR (2000). United Nations Sources and Effects of Ionizing Radiation. Volume I: Sources; Volume II: Effects. United Nations Scientific Committee on the Effects of Atomic Radiation, 2000 Report to the General Assembly, with scientific annexes. United Nations sales publications E.00.IX.3 and E.00. IX.4. United Nations, New York.